

Effect of platinum on the critical current density of fluorine-doped $\text{YBa}_2\text{Cu}_3\text{O}_x$ superconductors

TSUGIO HAMADA

Department of Electrical Engineering, Miyakonozyo College of Technology, 473-1 Yoshio, Miyakonozyo 885, Japan

YOSHIHISA OHZONO

Department of Electronic Engineering, Kagoshima University, 1-21-40 Koorimoto, Kagoshima 890, Japan

TADAIHIRO AKUNE, NOBUYOSHI SAKAMOTO

Department of Electrical Engineering, Kyushu Sangyo University, 2-3-1 Matsugadai, Higashi-ku, Fukuoka 813, Japan

The critical current density, J_c , in fluorine-doped $\text{YBa}_2\text{Cu}_3\text{O}_x$ bulk superconductors has been measured at several temperatures. The measured J_c value is 10^8 A m^{-2} at 77 K and 0.5 T. A sample with a larger critical current density can be produced by the addition of a small amount of platinum during the sintering process. The added platinum has the effect of evenly distributing Y_2BaCuO_5 particles and voids in the matrix in comparison with the undoped sample. These distributions of Y_2BaCuO_5 particles and voids are reflected in an increase in the critical current density. However, these distributions are not directly related to the observed peak effect in the critical current density. If the fluorine-doped $\text{YBa}_2\text{Cu}_3\text{O}_x$ superconductor consists of the matrix and a phase with a Ginzburg–Landau parameter, that is slightly different from that of the matrix, then the occurrence of the peak effect can be explained.

1. Introduction

A considerable amount of research has been performed on improving the critical current density-values in the cuprate based high T_c superconductors [1].

The critical current densities at 77 K in bulk high- T_c superconductors are inferior to those observed in the low- T_c metal superconductors although high values have been attained in quench and melt growth (QMG) processed $\text{YBa}_2\text{Cu}_3\text{O}_7$ samples and also in melt textured samples [2–4]. This success is achieved by introducing effective pinning centres into the superconductor. The dominant pinning centres in $\text{YBa}_2\text{Cu}_3\text{O}_7$ are induced by Y_2BaCuO_5 particles. However, Y_2BaCuO_5 particles are only produced at temperatures above 1000°C in QMG processed $\text{YBa}_2\text{Cu}_3\text{O}_7$ materials [5, 6]. It is not appropriate to utilize QMG processed materials in producing tapes or wires since silver material will melt during the high temperature processing. It is, therefore, important to decrease the synthesis temperature if we intend to produce high temperature superconductors with a large critical current density that can be used for industrial applications.

The present authors have attempted to decrease the synthesis temperature by fluorinating $\text{YBa}_2\text{Cu}_3\text{O}_x$ samples [7] and were able to decrease the synthesis temperature by about 100°C . The synthesized sample showed a microstructure similar to that produced by

the ordinary QMG processing [8]. However, the critical current density was inferior to that of the QMG processed material [9]. This is because, the Y_2BaCuO_5 particles in the fluorine-doped superconductors are larger than those in the QMG processed material, so the fluxoid are not effectively pinned and move with the Lorentz force [10]. Recently, the critical current density in fluorine-doped $\text{YBa}_2\text{Cu}_3\text{O}_x$ has been measured to be greater than 10^2 A cm^{-2} at 0.5 T and 77 K and a peak effect was observed in the high temperature regions (70 K and 77 K). The synthesis process of this material differs from an earlier synthesis process, where a small amount of platinum is added in order to study its effect on the microstructure of the matrix and the critical current density.

In this paper, we discuss why the critical current density in fluorine-doped superconductors increases and also present a possible mechanism for the peak effect in the critical current density. For this purpose, we utilize two samples which show a peak effect, one has a small amount of added platinum, the other is a pure sample. The critical current densities and the microstructures of the two samples are compared.

2. Experimental procedure

The samples used in this study were fluorine-doped $\text{YBa}_2\text{Cu}_3\text{O}_x$ superconductors. The $\text{YBa}_2\text{Cu}_3\text{O}_x$

superconductor is produced from Y_2O_3 , $BaCO_3$ and CuO , powders of 99.99% purity. The fluorine-doped $YBa_2Cu_3O_x$ samples were produced from two master compositions, $YBa_2Cu_3O_x$ and $YBa_2Cu_3F_{0.4}O_x$. The $YBa_2Cu_3F_{0.4}O_x$ was synthesized from Y_2O_3 , BaF_2 and CuO powders of 99.99% purity. After mixing, the component powders were calcined at $900^\circ C$ for 8 h in air and then cooled down to room temperature in the furnace. In addition, we added a small amount of platinum (0.3 wt %) to one of the fluorine-doped samples in order to study the influence of platinum on the microstructure of the matrix. The temperature in the furnace was measured using a platinum thermocouple. The chosen fluorine content was selected on the basis of an observed maximum in the hysteresis loop during magnetization measurements. The $YBa_2Cu_3F_{0.4}O_x + Pt(0.3 \text{ wt } \%)$ (sample 1) and $YBa_2Cu_3F_{0.4}O_x$ (sample 2) were sintered at a temperature of $950^\circ C$ for 2 h. They were then cooled to room temperature at a cooling rate of $2^\circ C$ per h. The magnetic characteristics were measured using a superconducting quantum interference device (SQUID) magnetometer. The critical current density, J_c , was estimated from d.c. magnetization measurements. The samples were then set in epoxy resin, and polished to a mirror finish to enable the microstructures of the samples to be examined using an optical microscope.

3. Results and discussion

The critical current densities in the samples were estimated from the magnetization curves. Figs. 1 (a and b) and 2 show the experimental magnetization curves for samples 1 and 2 at several temperatures. The magnetization curves for sample 1 at temperatures below 50 K show similar behaviour to that observed for Nb-Ti. However, it was difficult for the magnetic flux lines to penetrate into the superconductor at temperatures below 20 K because the maximum magnetic field of the superconducting magnet used in this work was 1 T. The magnetization curves for samples 1 and 2 in the high temperatures region are shown in Fig. 1 (a and b). The estimated critical current density for the applied magnetic field are shown in Figs. 3 and 4. The critical current densities of samples 1 and 2 at 77 K and 0.5 T were 1×10^8 and $3 \times 10^7 A m^{-2}$ respectively. In Fig. 3 at low temperatures the critical current densities for sample 1 decrease with an increase in the applied magnetic field.

However, at higher temperatures (70 and 77 K) the critical current densities increase with an increase in the applied magnetic field. The critical current density of sample 2 was measured at 77 K and is shown in Fig. 4. Each sample shows a peak maximum value at high temperatures and low magnetic fields. The critical current density in sample 2 is inferior to that of sample 1. Thus it would appear that the added platinum influences the value of the critical current density in sample 1. Thus we are interested in the microstructures of the samples that could explain this difference. Fig. 5 (a and b) shows the microstructures of samples 1 and 2 and the void distributions in the samples.

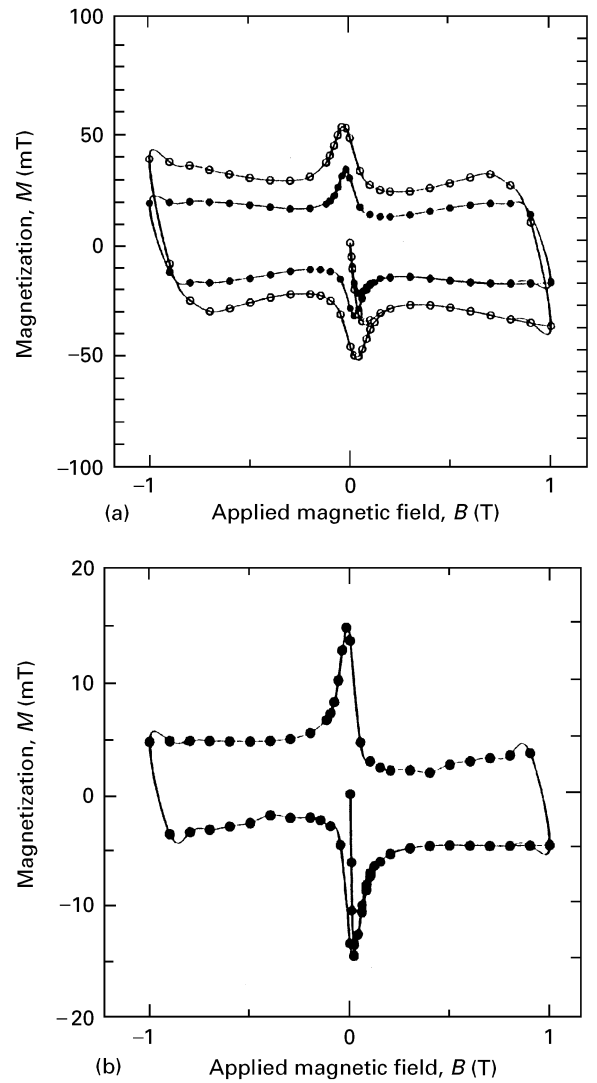


Figure 1 Anomalous magnetization curves for (a) sample 1 and (b) sample 2, at (●) 77 and (○) 70 K. Sample 1 which contains added platinum has a larger magnetization compared to the pure sample.

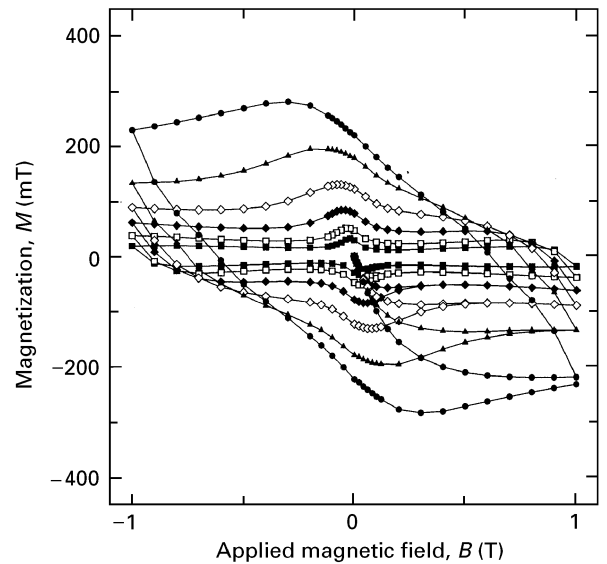


Figure 2 Magnetization curves for sample 1 in a magnetic field of up to 1 T at temperatures of; (■) 77 K, (□) 70 K, (◆) 60 K, (◇) 50 K, (▲) 40 K and (●) 30 K. The magnetization curves at temperatures below 50 K are similar to those for Nb-Ti at similar temperatures. However, the fluxoid do not penetrate into the superconductor at temperatures below 20 K.

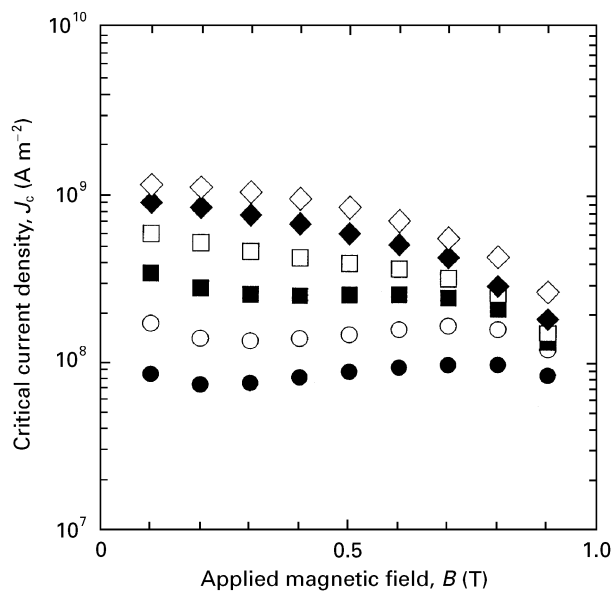


Figure 3 The magnetic field dependence of the critical current density for sample 1 at temperatures of; (●) 77 K, (○) 70 K, (■) 60 K, (□) 50 K, (◆) 40 K and (◇) 30 K. The critical current density shows a peak effect at temperatures of 70 and 77 K.

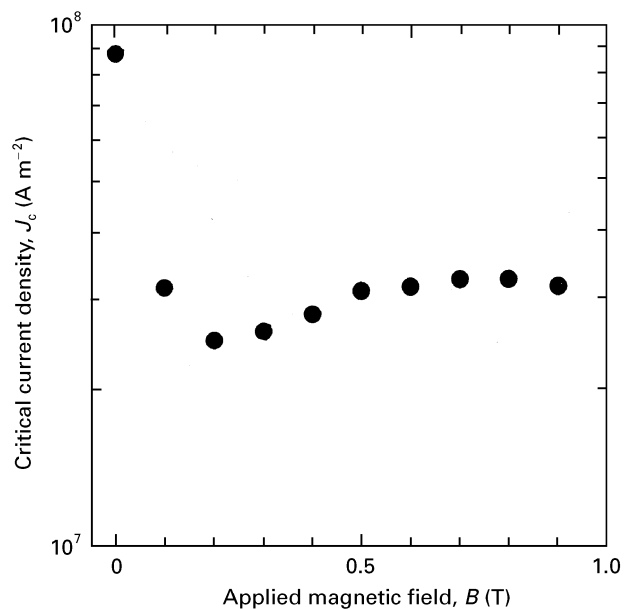


Figure 4 The magnetic field dependence of the critical current density at 77 K for sample 2. The critical current density shows a peak effect. However, its value is inferior to that in sample 1 and other fluorine-doped samples.

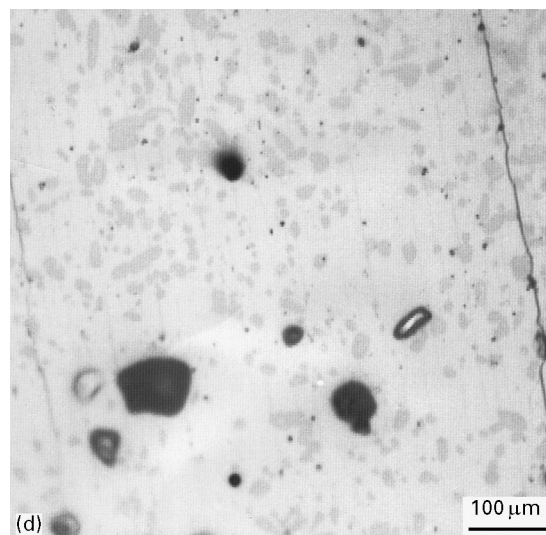
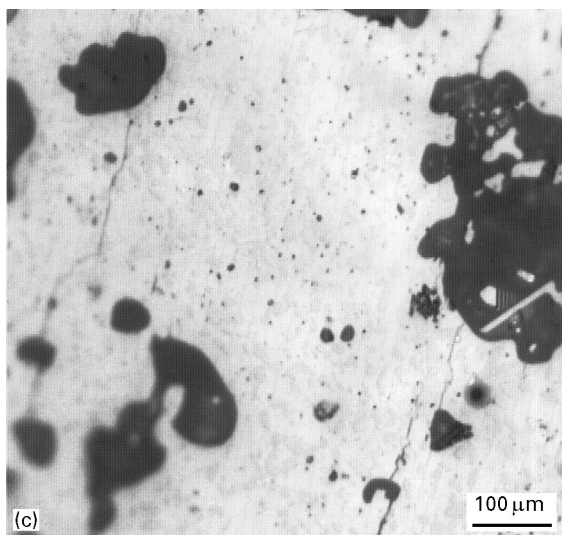
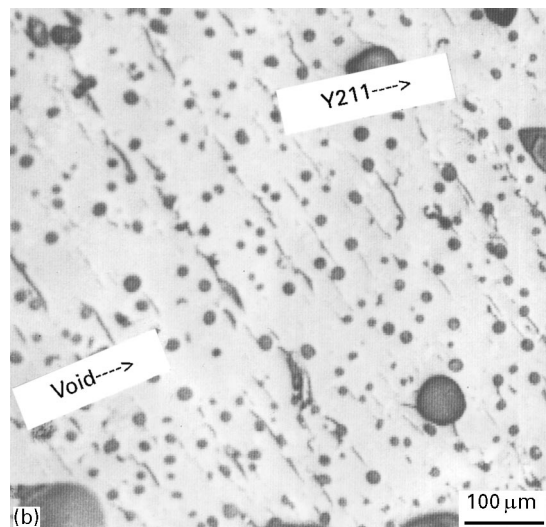
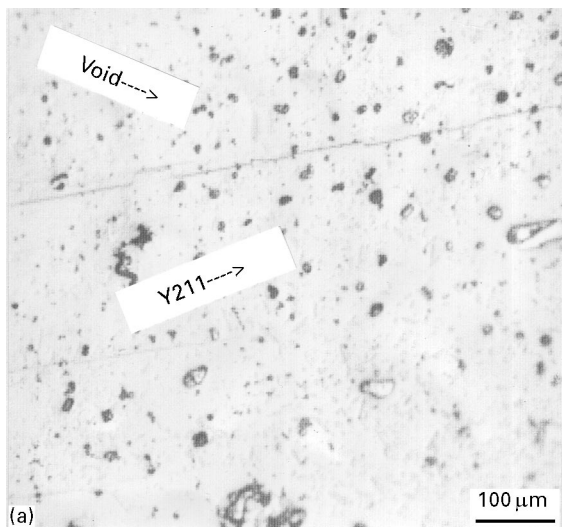


Figure 5 The microstructure observation of Y_2BaCuO_5 particles and voids in the matrix of (a) sample 1 and (b) sample 2. In the magnified micrographs, (c) the Y_2BaCuO_5 particles are more finely distributed in the matrix of sample 1 than (d) those of sample 2. The critical current density of sample 1 is greater than that of sample 2.

In sample 1 there are fine voids in the matrix, that are larger than those found in sample 2. The existence of Y_2BaCuO_5 particles in the samples cannot be observed with the same degree of clarity as the voids. Magnified micrographs of the samples are displayed in Fig. 5 (c and d).

In these micrographs it is possible to observe a large number of small Y_2BaCuO_5 grains in sample 1 as compared to the smaller number of larger grains present in sample 2. The critical current density can be considered as a balance between the Lorentz and pinning forces. Although the mechanism of the superconductivity in oxide superconductors is not currently fully understood, it is empirically known that the magnetic properties of these superconductors can be explained by the phenomenological Ginzburg–Landau theory. The superconductors are type-II superconductors with a small coherence length and a high Ginzburg–Landau parameter, κ , value. It can be expected, therefore, that the pinning mechanism in these superconductors can be described in terms of the Ginzburg–Landau theory as in the case of conventional low temperature superconductors. This can be expressed as follows:

$$F_p = J_c B \quad (1)$$

where F_p is the pinning force, J_c is the critical current density, and B is the applied magnetic field. When the Lorentz force equals the pinning force, the current density can be determined, and this current density is the critical current density in Equation 1. We assume that the fluxoid size is twice the coherence length (2ζ) in diameter and has no anisotropy. However, the value of the coherence length is given as the average value due to the anisotropic nature of the high-Ti superconductor. In the superconducting state, the energy is lower and more stable than in the normal state. The energy difference can be expressed as $B_c^2/2\mu_0$ where B_c is the thermodynamic critical field and μ_0 the permeability in a vacuum. If the normal particle has a diameter D , the loss in condensation energy when a fluxoid meets a normal particle is smaller than $(B_c^2/2\mu_0)\pi\zeta^2 D$ for each fluxoid. Thus, the elementary pinning force from the normal particles is approximately given by;

$$F_p = \frac{\pi\tau\zeta B_c^2}{4Da_f\mu_0} \left(1 - \frac{B}{B_{c2}}\right) \quad (2)$$

where a_f is the fluxoid spacing which is calculated as $a_f = (2\phi/(3)^{1/2}B)^{1/2}$, and τ is the volume fraction of the normal particles in the sample. It is found from Equation 2 that the pinning force becomes larger as D becomes smaller and τ increases. Thus, using these arguments we can explain why the platinum added sample has a large critical current density. Since the addition of the platinum to the sample results in a large number of small sized Y_2BaCuO_5 particles being produced.

This argument can explain the basic behaviour of the critical current density but we still need to explain the observed peak effect in the properties. We note that there is not a great deal of difference between

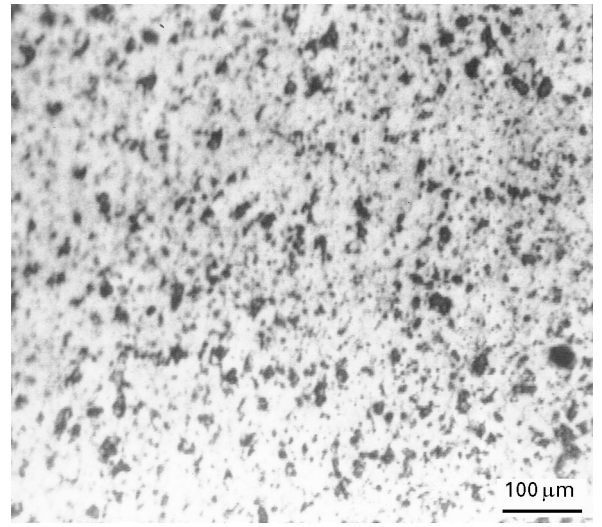


Figure 6 The microstructure of a fluorine-doped superconductor that did not show a peak effect in the critical current density. The distribution of voids is especially fine in comparison with that in samples 1 and 2.

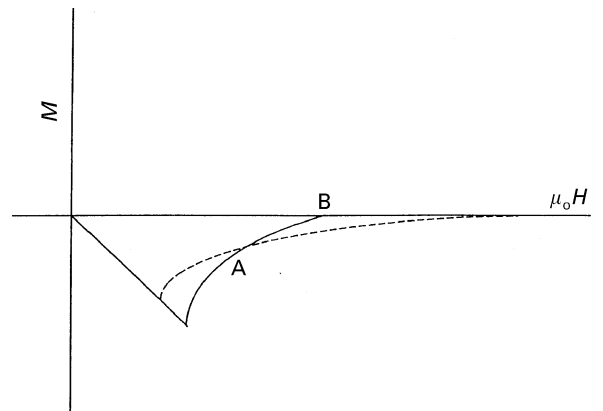


Figure 7 Schematic illustration of the peak effect produced by a sample with a slightly different Ginzburg–Landau parameter, κ , existing in the matrix. (—) magnetization of a phase with a slightly different κ value; (---) magnetization of the main matrix.

samples 1 and 2 with regard to the distribution of the voids and the Y_2BaCuO_5 particles. A micrograph of a sample that does not show a peak effect in the critical current density at high temperatures is shown in Fig. 6 [11]. In comparison with samples 1 and 2, the void distribution is finer than in the above two samples. It is thought that if the voids and/or Y_2BaCuO_5 particles are distributed finely and evenly in the matrix then the peak effect may not be observed. However since the critical current density is estimated from the magnetization curves the point that the magnetization of the sample could include contributions from regions of the matrix with slightly different Ginzburg–Landau parameters to that of the main matrix should be considered. If we assume that the pinning centre consists of a superconducting phase that has weaker superconducting properties than the main matrix phase then we predict that the peak effect will appear at the magnetic field where that weak phase changes into the normal state. Fig. 7 shows the magnetization curves for a material with the same thermodynamic critical magnetic field and a slightly different

Ginzburg–Landau parameter, κ , from that for the main matrix. The pinning force, expressed as a magnetic interaction, is proportional to the difference between the two magnetization curves in Fig. 7. Thus the force is equal to zero at point A and also at point B where the upper critical field of the pinning force becomes a maximum. One possible mechanism responsible for the creation of a slightly different κ parameter is the production of oxygen defects in the structure of the superconductor which is known to occur for $\text{YBa}_2\text{Cu}_3\text{O}_7$.

However, it is difficult to distinguish a Ginzburg–Landau parameter, κ , that is slightly different from that of the matrix. If the oxygen defects and their rates could be absolutely controlled then the above consideration could be experimentally tested. In fact, the oxide superconductor structures are considerably more complicated than the low- T_c metal superconductors. Therefore future investigations will be necessary to use the low- T_c metal superconductors to estimate the magnetic behaviours of the high- T_c superconductors [12]. This is because their structures are simple, and their electromagnetic properties can be accurately explained theoretically in low- T_c superconductors.

4. Conclusions

The critical current density in fluorine-doped $\text{YBa}_2\text{Cu}_3\text{O}_x$ superconductors has been measured at several temperatures. The reasons as to why the critical current density increases and a peak effect occurs have been investigated in terms of the microstructure and Ginzburg–Landau parameters. The results obtained in this study are;

(1) The addition of platinum into the fluorine-doped superconductors was more effective in producing small sized particles of Y_2BaCuO_5 and voids in the matrix as compared with the pure sample. This was reflected in the observed values of the critical current density.

(2) The distributions of the Y_2BaCuO_5 particles and voids were not directly related to the observed

peak effect. The existence of a phase with a Ginzburg–Landau parameter slightly different from the main matrix has been invoked to explain the peak effect.

Acknowledgements

The authors gratefully acknowledge Drs. M. Kashiwabara and T. Sakiyama for help with this work. We are also indebted to Drs. T. Toyohiro and Y. Hamada for the microstructural observations.

References

1. S. TANAKA and H. ITOZAKI, *Jpn. J. Appl. Phys.* **27** (1988) L622.
2. B. ROAS, L. SCHULTZ and G. ENDRES, *Appl. Phys. Lett.* **53** (1988) 1557.
3. K. WATANABE, H. YAMANE, H. KUROSAWA and Y. MUTO, *ibid.* **54** (1989) 575.
4. K. YAMAGUCHI, M. MUURAKAMI, H. FUJIMOTO, S. GOTOH, T. OYAMA, Y. SHIOHARA, N. KOSHIZUKA and S. TANAHKA, *J. Mater. Res.* **6** (1991) 1404.
5. K. SUGAWARA, D. J. BAAR, M. MURAKAMI, A. KONDOH, K. YAMAGUCHI, S. SHIOHARA and S. TANAKA, *Mod. Phys. Lett. B* **5** (1991) 1001.
6. H. FUJIMOTO, M. MURAKAMI, N. NAKAMURA, S. GOTOH, N. KOSHIZUKA and S. TANAKA, in Proceedings of the 4th International Symposium on Superconductivity (ISS91) Tokyo, Japan, October 1991 (Hong kong, Springer-Verlag, 1992).
7. T. HAMADA and R. MORIMO, *Phys. Stat. Sol. (a)* **145** (1994) 61.
8. T. HAMADA, R. MORIMO and S. OGURA, *J. Mater. Sci.* **31** (1996) 2579.
9. L. KLEIN, E. R. YACOBY and Y. YESHURUN, *Phys. Rev. B* **49** (1994) 4404.
10. M. DAEUMLING, J. M. SEUNTJENS and D. C. LARBALESTIER, *Nature* **346** (1990) 332.
11. T. HAMADA and T. NOMACHI, *Phys. Stat. Sol. (a)* **153** (1996) 165.
12. T. MATSUSHITA, E. S. OTABE and B. NI, *Supercond. Sci. Technol.* **5** (1992) S73.

*Received 23 February
and accepted 8 October 1996*